Anesthesiology 2005; 103:796–804

Inhibition of Kv4.3/KChIP2.2 Channels by Bupivacaine and Its Modulation by the Pore Mutation Kv4.3$_{V401I}$

Anna Solth, M.Sc., Cornelia C. Siebrands, M.Sc.,† Patrick Friederich, M.D.‡*

Background: **The transient outward current I_{to} is an important repolarizing K current in human ventricular myocardium mediated by Kv4.3 and KChIP2.2 subunits. Inhibition of I_{to} by amino-amide local anesthetics may be involved in severe cardiotoxic side effects. This study elucidates the molecular mechanisms of bupivacaine interaction with complexes formed by Kv4.3 and KChIP2.2 as well as the modulatory effect of KChIP2.2. For this purpose, the pharmacologic effects of bupivacaine on Kv4.3$_{wt}$/KChIP2.2 channels and on the pore mutant Kv4.3$_{V401I}$ were investigated.**

Methods: **Kv4.3/KChIP2.2 cDNA was transiently expressed in Chinese hamster ovary cells. Site-directed mutagenesis and patch clamp experiments were performed to analyze the effects of bupivacaine on wild-type and mutant channels.**

Results: **Inhibition of Kv4.3$_{wt}$/KChIP2.2 channels by bupivacaine was concentration-dependent and reversible. The IC_{50}s for inhibition of the charge conducted by Kv4.3$_{wt}$/KChIP2.2 channels by bupivacaine and levobupivacaine were 55 ± 8 and 50 ± 5 μM, respectively. The local anesthetic accelerated macroscopic current decline of Kv4.3$_{wt}$/KChIP2.2 and slowed recovery from inactivation without altering steady state inactivation. KChIP2.2 altered the response of Kv4.3$_{wt}$ channels to bupivacaine and bupivacaine modulated KChIP2.2 effects on Kv4.3$_{wt}$ channels. The pore mutation V401I slowed macroscopic current decline of Kv4.3 channels and recovery from inactivation, and it diminished modulation of gating by KChIP2.2. Bupivacaine inhibition of Kv4.3$_{V401I}$ resembled Kv4.3$_{wt}$ and was not changed by coexpression of KChIP2.2.**

Conclusions: **These results indicate that bupivacaine blocks Kv4.3/KChIP2.2 channels from the open state. They furthermore give structural evidence that amino-amide local anesthetics interfere with the effects of KChIP2.2 on Kv4.3 by an indirect mechanism.**

THE transient outward current I_{to} is an important repolarizing K current in the human heart.[1,2] The reduction of I_{to} contributes to prolongation of the cardiac action potential and ventricular arrhythmia occurring in ventricular failure[3,4] and in myocardial infarction.[5] Although the exact molecular composition of human I_{to} *in vivo* remains unclear,[6] it is widely accepted that Kv4.3 constitutes the principal α subunit in the human heart.[1,6–8] Kv4.3 α subunits coassemble with accessory subunits of the KChIP2 family (Kv channel interacting protein).[9,10] KChIP2 alters the level of surface expression as well as the gating properties of Kv4 channels.[11] The level of KChIP2 gene expression decreases from the epicardium to the endocardium and correlates with the transmural gradient of I_{to} in canine,[7,8] murine,[12] and human myocardium.[7,8] Knockout of the *KChIP2* gene in mice leads to a complete absence of I_{to}, a prolongation of action potential duration, and an increased susceptibility to development of polymorphic ventricular arrhythmia of the torsades de pointes type.[12] The precise mechanism of the interaction of KChIP with Kv4 channels has not been elucidated. However, it is clear that the N-terminal part of the Kv4.3 α subunit is crucial in binding and interacting with KChIP2.[11] The amino acids valine 399 and valine 401 in the inner pore region of Kv4.3 channels are also considered important for the modulatory effects of KChIP2.[13]

Inhibition of K channels by bupivacaine has been regarded as the molecular mechanism responsible for QTc interval prolongation of the electrocardiogram observed during toxic plasma concentrations of this amino-amide local anesthetic.[14–16] The pharmacologic effects of bupivacaine on cloned cardiac repolarizing K channel α subunits have been studied.[17–24] Also, the pharmacologic action of bupivacaine on some cardiac ion channel complexes formed from α and β subunits has been investigated.[18,22,24] The results of these studies demonstrate that amino-amide local anesthetics are not selective Na channel blockers but also block potassium channels in the same concentration range. In addition, these studies propose that amino-amide local anesthetics act as open channel blockers of Kv1.5 and Kv4.3 channels[17,20,24] and that local anesthetics interfere with the effects of KChIP on Kv4.3 channels by an unknown mechanism.[24]

I_{to} is suggested to constitute a potential molecular target involved in the cardiotoxic action of bupivacaine.[25,26] However, the effects of bupivacaine on complexes formed by human Kv4 and KChIP subunits have not yet been studied. Furthermore, it is unknown whether local anesthetics directly or indirectly interfere with the action of KChIP subunits by binding to the ion channel pore of Kv4.3 channels. Kv4.3 and KChIP2.2 constitute the most abundant isoforms of Kv4 and KChIP subunits present in human heart.[11,27] Therefore, this study was designed to investigate in detail bupivacaine effects on complexes formed by Kv4.3 and KChIP2.2 subunits cloned from human heart. Investigating the effects of bupivacaine on a pore mutation of Kv4.3 channels predicted to alter interaction with KChIP2.2[13]

* Research Student, † Ph.D. Student, Department of Anesthesiology and Institute for Neural Signal Transduction, ‡ Privatdozent, Department of Anesthesiology, University Medical Center Hamburg-Eppendorf.

Received from University Medical Center Hamburg-Eppendorf, Hamburg, Germany. Submitted for publication February 16, 2005. Accepted for publication June 21, 2005. Levobupivacaine and dextrobupivacaine were gifts from AstraZeneca, Södertalje, Sweden. Supported by the Deutsche Forschungsgemeinschaft, Bonn, Germany (Graduierten Kolleg 255, Neurale Signaltransduktion und deren pathologische Störungen and FR 1625/1-1). Ms. Solth and Ms. Siebrands contributed equally to this work.

Address reprint requests to Dr. Friederich: Department of Anesthesiology, University Medical Center Hamburg-Eppendorf, Martinistr. 52, 20251 Hamburg, Germany. Address electronic mail to: patrick.friederich@zmnh.uni-hamburg.de.

could also demonstrate whether bupivacaine and KChIP interfere by a direct or indirect mechanism.

Materials and Methods

Cell Culture

Chinese hamster ovary cells were cultured in 50-ml flasks (NUNC, Roskilde, Denmark) at 37°C in Minimum Essential Medium Alpha medium (GIBCO; Invitrogen, Carlsbad, CA) with 10% fetal calf serum (Biochrom, Berlin, Germany), 100 U/ml penicillin, and 100 mg/ml streptomycin (GIBCO) in a humidified atmosphere (5% CO_2). Cells were subcultured in 35-mm-diameter monodishes at least 1 day before transfection.

Molecular Biology and Transfection of Cells

The mutant $Kv4.3_{V401I}$ was created by site-directed mutagenesis. All constructs were cloned in the pcDNA3 expression vector. Chinese hamster ovary cells were transiently transfected with 0.1 μg $Kv4.3_{wt}$ (GenBank No. NM 004980) or $Kv4.3_{V401I}$ plasmid DNA, 1.0 μg KChIP2.2 plasmid DNA (GenBank No. NM 173191), 0.3 μg EFGP cDNA, and 3 μl lipofectamine reagent (GIBCO) per dish according to the manufacturer's protocol. Cells were cotransfected with an EGFP pcDNA3 construct to verify successful transfection. Only green fluorescing cells were used for patch clamp experiments. Patch clamp experiments were performed at room temperature 1–2 days after transfection.

Electrophysiology of Potassium Channels

Whole cell currents were measured with the patch clamp method[28] using an EPC-9 amplifier (HEKA Elektronik, Lambrecht, Germany) and Pulse software version 8.11 (HEKA Elektronik). Patch electrodes with a pipette resistance between 2.0 and 4.0 MΩ were pulled from borosilicate glass capillary tubes (World Precision Instruments, Saratoga, FL) and filled with the following solution: 160 mM KCl, 0.5 mM $MgCl_2$, 10 mM HEPES, 2 mM Na-ATP (all from Sigma, Deissenhofen, Germany); pH 7.2 (adjusted with KOH). The external solution applied on the cells was of the following composition: 135 mM NaCl, 5 mM KCl, 2 mM $CaCl_2$, 2 mM $MgCl_2$, 5 mM HEPES, 10 mM sucrose, 0.1 mg/ml Phenol red (all from Sigma); pH 7.4 (adjusted with NaOH). The capacity of the cells was 29.8 ± 16.1 pF (n = 20). Series resistance was 2.5–5 MΩ and actively compensated for by at least 80%. A p/4 leak subtraction protocol was used in the study. Bupivacaine (Sigma), levobupivacaine (AstraZeneca, Södertalje, Sweden), and dextrobupivacaine (AstraZeneca) were dissolved in the extracellular solution. The drugs were superfused on the cells by a hydrostatically driven perfusion system.

The holding potential of the cell membrane was −80 mV, and Kv4.3 channels were activated by different protocols. For channel stimulation by the rectangle pulse protocol, the membrane was hyperpolarized for 200 ms to −100 mV and subsequently depolarized to +40 mV for 1,000 ms. Current activation was analyzed by depolarization of the membrane potential for 1,000 ms from −40 to +60 mV in 10-mV steps. Steady state inactivation was measured by depolarizing the membrane to +40 mV for 25 ms from prepulses of a duration of 4,000 ms increasing from −75 and −15 mV in steps of 5 mV. For measuring the recovery from inactivation, the initial depolarization of the membrane potential to +40 mV for 1,500 ms was followed by depolarizing the membrane potential to −80 mV for different duration of time increasing from 10 to 5,120 ms by doubling the time spent at −80 mV (Δt) after each individual depolarization. The repolarization was followed by a depolarizing step of 25 ms to + 40 mV. Experiments were performed at room temperature. The recorded signal was filtered at 2 kHz and stored on a personal computer for later analysis with a sampling rate of up to 20 kHz.

Data Analysis

The current–time relation observed with the different protocols for potassium channel activation was used to determine the maximal outward current (I_{max}) as well as to quantify the charge (Q) crossing the membrane during the duration of the depolarization induced by the rectangle protocol. The charge crossing the membrane is equivalent to the time integrals of current traces and was determined using Pulse software version 8.11 (HEKA Elektronik). Inhibition was quantified by the ratio of time integrals of current traces in the presence of the drug to the mean of the time integrals before application of the drug and after washout of the drug (inhibition $Q = 1 - Q_{drug}/[(Q_{control} + Q_{washout})/2]$). The concentration–response curves were fitted with the Hill equation $e/e_{max} = 1/[1 + (IC_{50}/c)^{\gamma}]$ using nonlinear regression (e = effect, e_{max} = maximal effect, c = anesthetic concentration, γ = Hill coefficient, and IC_{50} = concentration of half-maximal effect). Regression analysis was performed using Kaleidagraph (Synergy Software, Reading, PA). The whole cell conductance G_{max} was calculated using the following formula: $G_{max} = I_{max}/(V_m - E_K)$, where I_{max} is the maximum current during each test potential, V_m is the membrane potential, and E_K is the Nernst potential for potassium (−87.54 mV under our experimental conditions). The means of the whole cell conductance were mathematically described by a Boltzmann function $G = G_{max}/[1 + \exp((V_{0.5} - V_m)/k)]$, where G_{max} is the maximal whole cell conductance, $V_{0.5}$ is the voltage of half-maximal activation, V_m is the membrane potential, and k is the slope factor, using Kaleidagraph software. Time-dependent inactivation was mathematically described using a biexponential function $y = C + A_1\exp(-t/\tau_1) + A_2\exp(-t/\tau_2)$, where τ_1 and τ_2 are the system time constants, A_1 and A_2 are the amplitudes

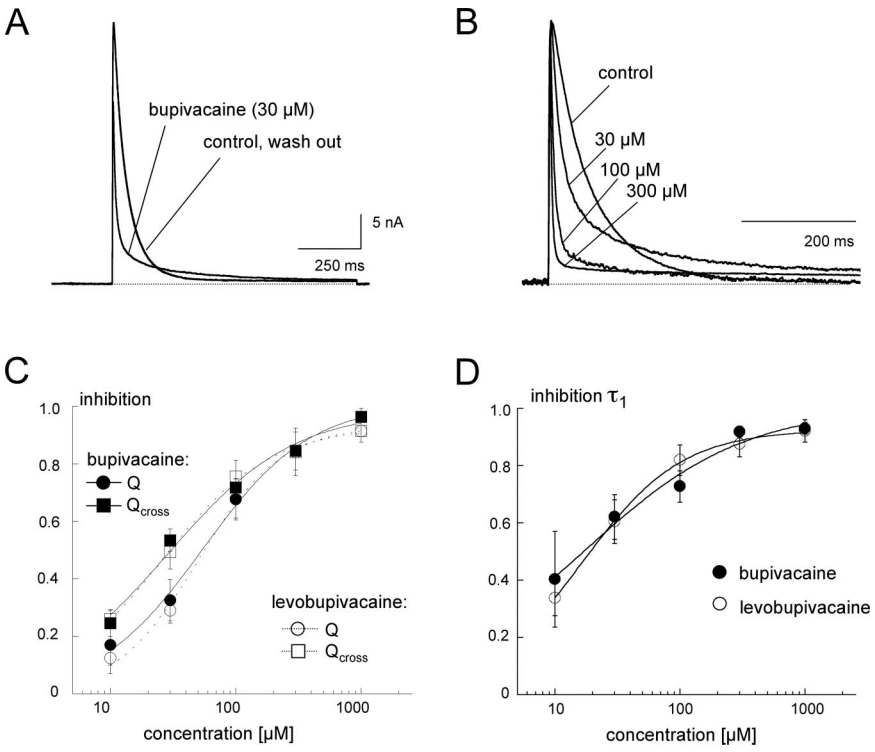

Fig. 1. (*A*) Original current traces evoked by a 1-s pulse to +40 mV, showing the effects of 30 μM bupivacaine on $Kv4.3_{wt}$/KChIP2.2 channels. The current was reduced and its shape was altered, resulting in a crossing of the currents under drug conditions with the currents under control and washout conditions. (*B*) Effects of different bupivacaine concentrations on $Kv4.3_{wt}$/KChIP2.2. Currents were normalized to the maximum to show the alteration of the current shape as well as the times of crossing for the different concentrations. (*C*) The inhibition of the $Kv4.3_{wt}$/KChIP2.2 channels was quantified as the inhibition of the charge transfer through $Kv4.3_{wt}$/KChIP2.2 (Q) during the entire protocol and as inhibition of the charge transfer only until the crossing of currents was reached (Q_{cross}). These two parameters of inhibition were plotted *versus* the concentration and fitted using Hill equations (n = 3–10 for each concentration). (*D*) The local anesthetic accelerated the fast time constant τ_1 of $Kv4.3_{wt}$/KChIP2.2 inactivation. This effect was quantified as inhibition of τ_1 (see Materials and Methods), and the concentration–response curve of inhibition of τ_1 was fitted with a Hill equation (n = 3–10 for each concentration).

of each component of the exponential, and C is the baseline value. Recovery from inactivation was determined by relating the maximal size of the outward current during the test pulse to the size of maximal outward current during the prepulse. The time-dependent increase of this ratio was mathematically described with a monoexponential or biexponential function as described above. The time course of the development of block was analyzed using the following equation: $y = (I_{control} - I_{drug})/I_{control}$, where $I_{control}$ is the current at any given time under control conditions and I_{drug} is the current at the same time under drug conditions. Data points are presented as mean ± SD unless stated otherwise. Statistical significance was tested using analysis of variance and the Tukey-Kramer multiple comparisons test (Graph Pad; Prism, San Diego, CA) or two-sided paired and unpaired Student *t* tests as appropriate (Excel; Microsoft, Redmond, WA). A value of $P < 0.05$ was regarded as significant. The number n is the number of experiments.

Results

$Kv4.3_{wt}$/KChIP2.2 currents activated with a midpoint of 0 ± 4 mV (n = 10) and were fully activated at a potential of +40 mV. Therefore, a rectangle protocol with a depolarization to +40 mV was chosen to test the influence of bupivacaine and levobupivacaine on the channel complexes. The rectangle protocol evoked a rapidly activating and inactivating A-type current (fig. 1A). Bupivacaine (30 μM) had two effects on the $Kv4.3_{wt}$/KChIP2.2 current. It reduced the current, and it accelerated macroscopic current decline in a such way that a crossing phenomenon occurred upon overlay of control and drug traces. Both effects were reversible upon washout (fig. 1A). The current decline of $Kv4.3_{wt}$/KChIP2.2 currents was described using two time constants. Bupivacaine, 30 μM, reduced the fast time constant τ_1 from 35 ± 14 ms (n = 9) to 10 ± 3 ms (n = 5; $P < 0.01$), and it increased the slow time constant τ_2 from 96 ± 44 ms (n = 9) to 147 ± 37 ms (n = 5; $P < 0.05$). The ratio of the amplitudes of the time constants, amplitude 1 and amplitude 2, was changed by bupivacaine from 62 ± 14% for amplitude 1 and 38 ± 14% for amplitude 2 under control and washout conditions to 80 ± 5% for amplitude 1 and 20 ± 5% for amplitude 2 when 30 μM bupivacaine was applied (n = 5; $P < 0.05$). This resulted in the crossing phenomenon. Consequently, bupivacaine action on the channel complex was inhibitory before the crossing but stimulatory after the crossing of currents.

Figure 1B shows the effect of different concentrations of bupivacaine on the $Kv4.3_{wt}$/KChIP2.2 channel complex. The reduction of current and the change of current shape were concentration dependent. The inhibition of $Kv4.3_{wt}$/KChIP2.2 channels was quantified as reduction of the charge transfer through $Kv4.3_{wt}$/KChIP2.2 channels during the entire time of the depolarization (Q) as well as reduction of the charge transfer from the beginning of the depolarization until the crossing of currents (Q_{cross}). The concentration–response data were mathematically described with Hill functions (fig. 1C). The

Table 1. Parameters of Hill Functions

	Inhibition Q Bupivacaine	Inhibition Q Levobupivacaine	Inhibition Q_{cross} Bupivacaine	Inhibition Q_{cross} Levobupivacaine	Acceleration τ_1 Bupivacaine	Acceleration τ_1 Levobupivacaine
e_{max}, %	101 ± 5	93 ± 3	99 ± 7	93 ± 2	100 ± 9	93 ± 1
Hill	1.02 ± 0.12	1.31 ± 0.14	0.88 ± 0.18	1.01 ± 0.08	0.68 ± 0.24	1.09 ± 0.06
IC_{50}, μM	55.0 ± 8.2	50.4 ± 5.1	29.7 ± 6.9	25.8 ± 2.0	17.2 ± 5.8	16.6 ± 0.7
n	20	26	24	28	26	29

Parameters of the Hill function describing concentration-dependent inhibition of charge (Q), charge until crossing (Q_{cross}), and fast time constant of current delay (τ_1) of Kv4.3/KChIP2.2 channels by bupivacaine and levobupivacaine. Data are presented as mean ± SEM.

e_{max} = maximal effect; Hill = Hill coefficient; IC_{50} = concentration of half-maximal inhibition; n = number of experiments.

IC_{50} values for inhibition of Q, and Q_{cross} by bupivacaine were 55 ± 8 μM (n = 20) and 30 ± 7 μM (n = 24), respectively (table 1). The acceleration of macroscopic current decline was concentration-dependent as well, and the time until the crossing occurred increased with concentration (fig. 1B). The Hill function describing the concentration–response data for reduction of τ_1 yielded an IC_{50} value of 17 ± 6 μM (n = 26) (fig. 1D and table 1). Although τ_2 was increased by 30 μM bupivacaine, it was impossible to be analyzed under higher drug concentrations (300 μM and 1 mM) because of the small size of the residual current. Levobupivacaine had similar effects on $Kv4.3_{wt}$/KChIP2.2. The IC_{50} values for inhibition of Q, Q_{cross}, and reduction of τ_1 by levobupivacaine were 50 ± 5 μM (n = 26), 26 ± 2 μM (n = 28), and 17 ± 1 μM (n = 29), respectively (table 1). There was no significant difference in any parameter of $Kv4.3_{wt}$/KChIP2.2 inhibition by racemic bupivacaine and by levobupivacaine ($P > 0.05$).

To further analyze the possible stereospecific effect of bupivacaine, paired tests were performed with the pure enantiomers *S*(−)-levobupivacaine and *R*(+)-dextrobupivacaine at a concentration of 30 μM. This concentration was chosen because it was near the IC_{50} value for the inhibition of Q and hence at the steepest part of the concentration–response curve. A gentle difference in potency between the enantiomers should best be detectable at this part of the concentration–response curve. Levobupivacaine and dextrobupivacaine inhibited Q at 30 μM with nearly identical potencies (levobupivacaine: 51.4 ± 1%, dextrobupivacaine: 50.5 ± 1%; n = 11; $P > 0.05$). Therefore, only racemic bupivacaine was used in the following experiments.

To establish the effect of bupivacaine on $Kv4.3_{wt}$/KChIP2.2 channel gating, the effects of 100 μM bupivacaine on voltage-dependent activation, steady state inactivation, and recovery from inactivation were investigated (figs. 2 and 3). Bupivacaine affected voltage-dependent activation as well as recovery from inactivation without changing steady state inactivation. Figure 2 shows original current traces elicited by the activation protocol (fig. 2A), the inactivation protocol (fig. 2B), and the recovery protocol (fig. 2C). Application of 100 μM bupivacaine reduced the current during every protocol. This effect was always reversible upon washout. Bupivacaine (100 μM) modulated the voltage dependence of activation by shifting the midpoint of current activation in the depolarizing direction by 10 ± 4 mV (n = 5; $P < 0.05$). The slope of the activation curve was increased by 2 ± 1 mV (n = 5; $P < 0.05$; fig. 3A and table 2). The

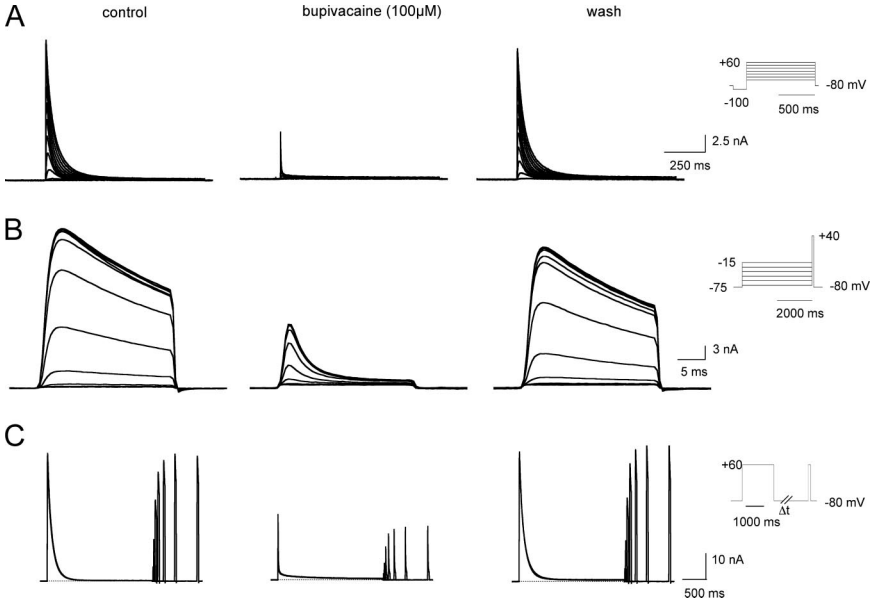

Fig. 2. Original current traces demonstrating bupivacaine effects on different $Kv4.3_{wt}$/KChIP2.2 gating parameters. The influence of bupivacaine on activation (*A*), inactivation (*B*), and recovery from inactivation (*C*) was studied using the appropriate pulse protocols depicted as an *inset* next to the traces. Shown are currents under control conditions, after application of 100 μM bupivacaine, and after the washout of the substance. All currents were reduced by bupivacaine.

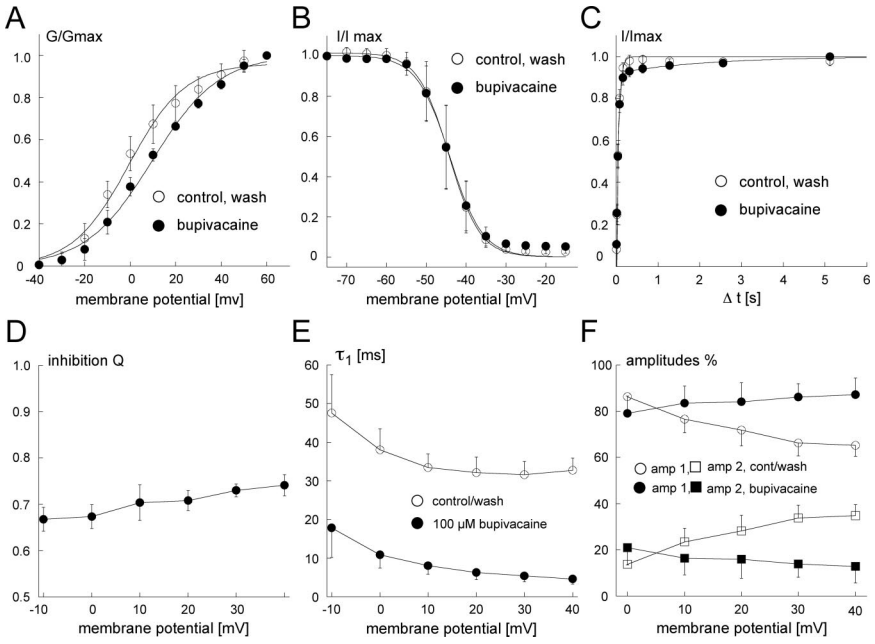

Fig. 3. (*A*) Bupivacaine (100 μM) shifted the voltage dependence of Kv4.3$_{wt}$/KChIP2.2 activation to more depolarized potentials and increased the slope factor, which resulted in a steeper rise of the conductance–voltage curve under bupivacaine than under control and washout conditions. (*B*) The voltage dependence of channel inactivation was not altered by bupivacaine (100 μM). (*C*) The recovery from inactivation was slowed by bupivacaine (100 μM). Under control and washout conditions, one time constant was sufficient to describe the conductance–time relation of recovery from inactivation adequately, but two time constants were necessary to describe this curve when bupivacaine was applied (see also table 2). (*D* and *E*) Voltage dependence of the bupivacaine (100 μM) effects. (*D*) Inhibition of Q increased with voltage in the range from −10 to +40 mV. (*E*) The fast time constant of inactivation was voltage dependent under control and washout as well as under drug conditions. (*F*) The distribution of the amplitudes was voltage dependent under control and washout conditions. At 0 mV, the amplitude of the fast time constant of inactivation (amplitude 1) was much larger than amplitude 2. Toward more positive potentials, the curves for both amplitudes were converging. This voltage dependence was reversed by 100 μM bupivacaine, with amplitude disparity becoming more marked with voltage.

voltage dependence of inactivation was not altered by 100 μM bupivacaine (fig. 3B). However, the local anesthetic slowed the recovery from inactivation (fig. 3C). Under control and washout conditions, the time dependence of the recovery from inactivation was adequately fitted with one time constant (τ_{rec}, 57 ± 7 ms; n = 6). Application of 100 μM bupivacaine altered Kv4.3/KChIP2.2 gating in such a way that two time constants were necessary to adequately describe the time dependence of recovery (τ_{rec1} = 42 ± 6 ms, τ_{rec2} = 2,339 ± 728 ms; n = 6). Both time constants differed significantly from the time constant under control and washout conditions ($P < 0.05$; table 2)

Table 2. Effect of Bupivacaine on Channel Gating

	Control/Washout	100 μM Bupivacaine
Activation		
$V_{0.5}$, mV	−0.1 ± 3.8	9.6 ± 2.0
Slope factor, mV	12.4 ± 2.6	14.6 ± 1.6
G_{max}, %	96.9 ± 1.9	100.4 ± 0.9
n	5	5
Voltage-dependent inactivation		
$V_{0.5}$, mV	−44.4 ± 2.7	−44.1 ± 3.0
Slope factor, mV	−3.4 ± 0.3	−3.7 ± 0.3
G_{max}, %	101.0 ± 1.2	100.0 ± 0.8
n	4	4
Recovery from inactivation		
τ_{rec1}, ms	57.2 ± 7.0	41.7 ± 5.6
τ_{rec2}, ms		2,338.5 ± 728.1
n	6	6

Bupivacaine (100 μM) induced effects on the voltage dependence of activation, voltage dependence of inactivation, and recovery from inactivation of Kv4.3/KChIP2.2. Data are presented as mean ± SD.

$V_{0.5}$ = voltage of half-maximal activation; G_{max} = maximal conductance; n = number of experiments; τ_{rec} = time constant of recovery.

Voltage dependence of Kv4.3$_{wt}$/KChIP2.2 block was analyzed as the inhibition of Q. Inhibition of Q by 100 μM bupivacaine increased between membrane potentials of −10 and +40 mV in a voltage-dependent manner (fig. 3D; $P < 0.05$, tested by analysis of variance). At −10 mV, inhibition of Q was 67 ± 3% whereas at +40 mV, Q was inhibited by 74 ± 2% (n = 4). The fast time constant of current decline (τ_1) was inversely related to voltage under control as well as under bupivacaine (100 μM) conditions (fig. 3E; $P < 0.05$, tested by analysis of variance). Under control conditions, τ_1 was 48 ± 10 ms at −10 mV and 33 ± 3 ms at +40 mV (n = 4). When bupivacaine was applied, τ_1 was 18 ± 8 ms at −10 mV and decreased to 5 ± 1 ms at +40 mV (n = 4; fig. 3E). Because it was not always possible to describe the inactivation process with two time constants at −10 mV, the voltage dependence of the amplitudes was analyzed between membrane potentials of 0 mV and +40 mV. The distribution of the amplitudes of the fast and the slow time constant of current decline was voltage-dependent under control and washout conditions (fig. 3F), with values of 86 ± 9% for amplitude 1 and 14 ± 9% for amplitude 2 at 0 mV and 65 ± 5% for amplitude 1 and 35 ± 5% for amplitude 2 at +40 mV. Application of 100 μM bupivacaine reversed voltage dependence of distribution of the amplitudes, with an amplitude 1 of 79 ± 7% at 0 mV and 87 ± 7 at +40 mV (n = 4; $P < 0.05$).

To gain further insight into the mechanism of Kv4.3 inhibition by bupivacaine, we in addition analyzed the pore mutant Kv4.3$_{V401I}$. The electrophysiologic properties of this pore mutant were characterized first. Figures

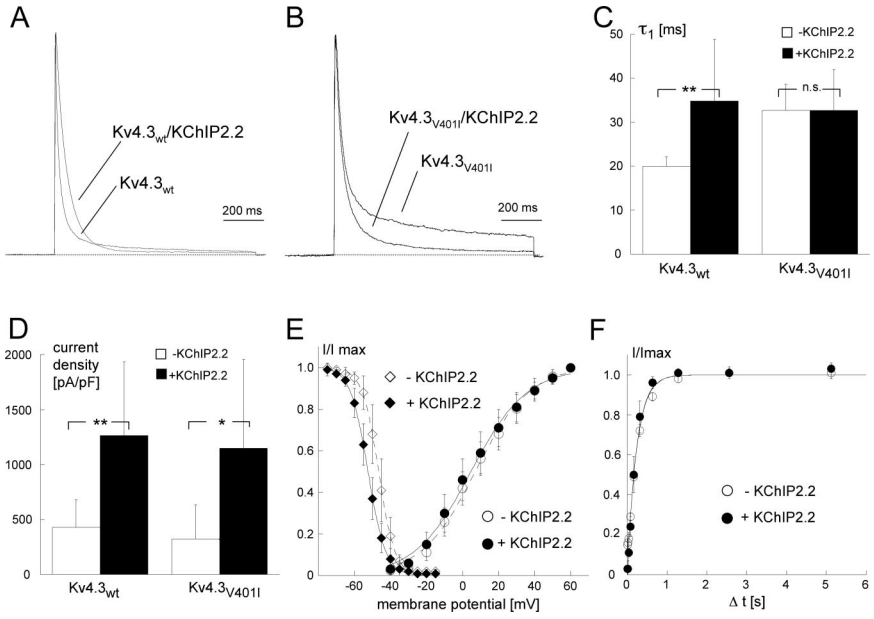

Fig. 4. (*A*) Overlay of normalized currents through Kv4.3$_{wt}$ and Kv4.3$_{wt}$/KChIP2.2. (*B*) Overlay of normalized currents through Kv4.3$_{V401I}$ and Kv4.3$_{V401I}$/KChIP2.2. (*C*) The mutant channel Kv4.3$_{V401I}$ showed a slowed macroscopic current decline compared with Kv4.3$_{wt}$. KChIP2.2 had no effect on τ_1 of Kv4.3$_{V401I}$. (*D*) Current density of wild-type and mutant Kv4.3 channels was significantly increased by coexpression of KChIP2.2. (*E*) Voltage dependence of steady state inactivation (◇, ◆) and activation (○, ●) of Kv4.3$_{V401I}$ (*open symbols*) and Kv4.3$_{V401I}$/KChIP2.2 channel complexes (*filled symbols*). (*F*) Recovery from inactivation of Kv4.3$_{V401I}$ and Kv4.3$_{V401I}$/KChIP2.2 channel complexes. * $P < 0.05$; ** $P < 0.01$.

4A and B show normalized currents through Kv4.3 wild-type and mutant channels expressed with and without KChIP2.2. For Kv4.3$_{wt}$, a crossing of current traces with and without KChIP is observed (fig. 4A). In contrast, no such crossing is found for Kv4.3$_{V401}$ (fig. 4B). The mutant channel Kv4.3$_{V401I}$ exhibited a slower macroscopic current decline than Kv4.3$_{wt}$ (figs. 4A and B). τ_1 was 20 ± 2 ms (n = 10) for Kv4.3$_{wt}$ and 33 ± 6 ms (n = 7) for Kv4.3$_{V401I}$ ($P < 0.01$; fig. 4C and table 3). The slow time constant τ_2 was also slowed by the mutation (130 ± 25 ms for Kv4.3$_{wt}$, n = 10, *vs.* 293 ± 48 ms for Kv4.3$_{V401I}$, n = 7; $P < 0.01$; table 3). KChIP2.2 reduced τ_2 but had no effect on the fast time constant of Kv4.3$_{V401I}$ current decline (figs. 4B and C and table 3). KChIP2.2 increased the current density of both Kv4.3$_{wt}$ as well as Kv4.3$_{V401I}$ channels (fig. 4D). Current densities did not significantly differ between Kv4.3$_{wt}$ and Kv4.3$_{V401I}$. This was also the case for Kv4.3$_{wt}$ and Kv4.3$_{V401I}$ when expressed in combination with KChIP2.2 (fig. 4D). The voltage dependence of activation and inactivation of Kv4.3$_{V401I}$ were similar to Kv4.3$_{wt}$. The voltage dependence of inactivation was shifted to more negative potentials by coexpression with KChIP2.2 (fig. 4E; activation: $V_{0.5}$ = 7.7 ± 6.0 mV for Kv4.3$_{V401I}$, n = 9, and $V_{0.5}$ = 6.0 ± 7.4 mV for Kv4.3$_{V401I}$/KChIP2.2, n = 7, $P > 0.05$; inactivation: $V_{0.5}$ = −46.6 ± 2.6 mV for Kv4.3$_{V401I}$, n = 7, and $V_{0.5}$ = −52.6 ± 2.0 mV for Kv4.3$_{V401I}$/KChIP2.2, n = 6; $P < 0.05$). The mutation significantly slowed the recovery from inactivation of Kv4.3 channels (compare figs. 3C and 4F). Coexpression of KChIP2.2 did not significantly change the time constants of recovery from inactivation (fig. 4F; τ_{rec} = 250 ± 19 ms for Kv4.3$_{V401I}$, n = 5, and τ_{rec} = 240 ± 48 ms for Kv4.3$_{V401I}$/KChIP2.2, n = 5; $P > 0.05$).

To investigate whether the accessory β subunit KChIP2.2 modulates bupivacaine sensitivity of Kv4.3 channels, the inhibition of Kv4.3$_{wt}$/KChIP2.2 channel complexes by bupivacaine (30 μM) was compared with the inhibition of Kv4.3$_{wt}$ channels expressed without

Table 3. Comparison of Current Decay between Kv4.3$_{wt}$ and Kv4.3$_{V401I}$

	Kv4.3$_{wt}$	Kv4.3$_{wt}$/KChIP2.2	Kv4.3$_{V401I}$	Kv4.3$_{V401I}$/KChIP2.2
Control				
τ_1, ms	20 ± 2	35 ± 14	33 ± 6	33 ± 9
τ_2, ms	130 ± 25	96 ± 44	293 ± 48	196 ± 49
Amplitude 1, %	84 ± 6	61 ± 13	83 ± 4	85 ± 5
Amplitude 2, %	16 ± 6	39 ± 13	17 ± 4	15 ± 5
n	10	9	7	9
30 μM bupivacaine				
τ_1, ms	9 ± 2	10 ± 3	22 ± 6	9 ± 2
τ_2, ms	90 ± 14	147 ± 37	238 ± 53	139 ± 47
Amplitude 1, %	79 ± 6	80 ± 5	75 ± 6	83 ± 3
Amplitude 2, %	21 ± 6	20 ± 5	25 ± 6	17 ± 3
n	10	5	7	9

Time constants (τ) and amplitudes for biexponential fit of current decay of Kv4.3 channels under control conditions and under bupivacaine (30 μ_m). Data are presented as mean ± SD.

n = number of experiments.

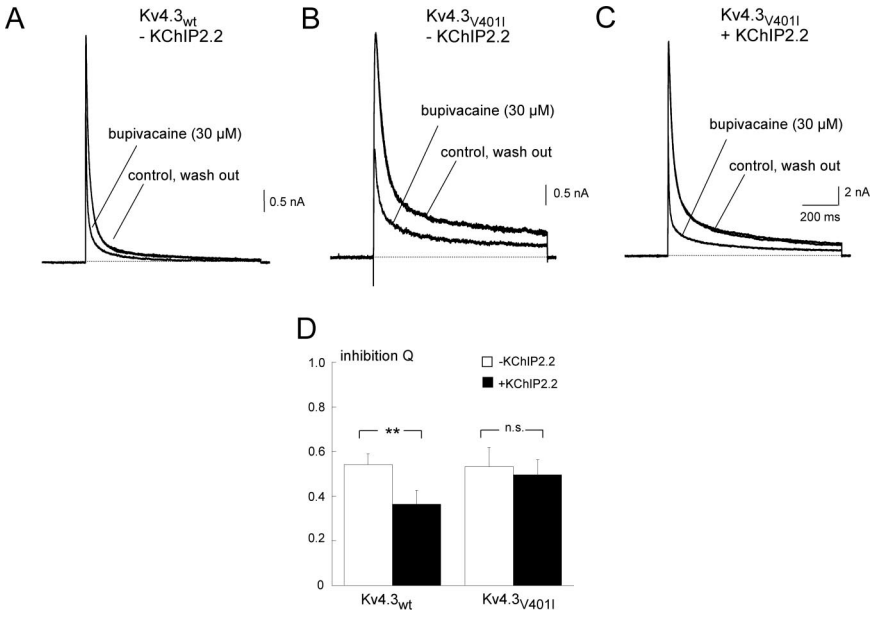

Fig. 5. (*A–C*) Original current traces through $Kv4.3_{wt}$, $Kv4.3_{V401I}$, and $Kv4.3_{V401I}$/KChIP2.2 channels. $Kv4.3_{V401I}$ shows a slowed macroscopic current decline compared with $Kv4.3_{wt}$. Note the different y-scales, indicating that $Kv4.3_{V401I}$/KChIP2.2 generated currents with a larger amplitude than $Kv4.3_{wt}$ and $Kv4.3_{V401I}$. Bupivacaine, 30 μM, inhibited all three channels but did not induce a crossing of any current. (*D*) Inhibition of Q by 30 μM bupivacaine was significantly reduced when $Kv4.3_{wt}$ channels where coexpressed with KChIP2.2. This KChIP2.2 effect was not observed when $Kv4.3_{V401I}$ was coexpressed with KChIP2.2. * $P < 0.05$; ** $P < 0.01$.

the β subunit as well as with inhibition of the pore mutant $Kv4.3_{V401I}$ expressed with and without KChIP2.2 (figs. 5A–C). Bupivacaine (30 μM) inhibited $Kv4.3_{wt}$, $Kv4.3_{V401I}$, and $Kv4.3_{V401I}$/KChIP2.2 channels (figs. 5A–C). However, in contrast to $Kv4.3_{wt}$/KChIP2.2, bupivacaine did not induce a crossing phenomenon in $Kv4.3_{wt}$, $Kv4.3_{V401I,}$ or $Kv4.3_{V401I}$/KChIP2.2 channels (compare figs. 5A–C with fig. 1A). As a consequence, inhibition (Q) of $Kv4.3_{wt}$/KChIP2.2 was significantly less than inhibition (Q) of $Kv4.3_{wt}$ (36 ± 6% for $Kv4.3_{wt}$/KChIP2.2, n = 5, *vs.* 54 ± 5% for $Kv4.3_{wt}$, n = 10; $P < 0.01$; fig. 5D). The reduction of bupivacaine sensitivity of $Kv4.3_{wt}$ by KChIP2.2 was not observed with the pore mutant $Kv4.3_{V401I}$. Inhibition (Q) of $Kv4.3_{V401I}$ amounted to 53 ± 9% (n = 6) in the absence of KChIP2.2, and it was 50 ± 7% (n = 7) in the presence of KChIP2.2 ($P > 0.05$; fig. 5D). Inhibition of $Kv4.3_{V401I}$ and $Kv4.3_{wt}$ channels did not significantly differ ($P > 0.05$; fig. 5D). KChIP2.2 slowed the development of block by bupivacaine of $Kv4.3_{wt}$ channels but not of $Kv4.3_{V401I}$ channels. The time constant for the development of $Kv4.3_{wt}$ block was 3 ± 1 ms (n = 6), 6 ± 1 ms for $Kv4.3_{wt}$/KChIP2.2 (n = 5), 4 ± 1 ms for $Kv4.3_{V401I}$ (n = 6), and 4 ± 1 ms for $Kv4.3_{V401I}$/KChIP2.2 (n = 8). Block of both $Kv4.3_{V401I}$ and $Kv4.3_{V401I}$/KChIP2.2 channels developed significantly slower than block of $Kv4.3_{wt}$/KChIP2.2 channels ($P < 0.01$).

Discussion

This study established the effects of the local anesthetic bupivacaine on $Kv4.3_{wt}$/KChIP2.2 and $Kv4.3_{V401I}$/KChIP2.2 channel complexes expressed in Chinese hamster ovary cells. The biophysical properties of the wild-type ion channel complex were in accord with biophysical properties of Kv4/KChIP2 channel complexes reported previously.[11,13] The local anesthetics bupivacaine and levobupivacaine reduced $Kv4.3_{wt}$/KChIP2.2 currents in a concentration-dependent and reversible manner. Both drugs exhibited the same effects on $Kv4.3_{wt}$/KChIP2.2 and did not differ with regard to inhibitory potency. Bupivacaine caused a depolarizing shift of voltage-dependent current activation. The local anesthetic decreased the time constants of macroscopic current decline, slowed recovery from channel inactivation, and induced a crossing phenomenon of currents.

Acceleration of macroscopic current decline is a characteristic feature of open channel block.[29,30] This mechanism has already been described previously for the inhibition of several Kv α subunits, including Kv4.3 by bupivacaine.[17,19,20,31,32] Inhibition of Kv1.5 channels by bupivacaine is mediated by threonine 477 (current number according to GenBank No. NM 002234: T479) within the tetraethylammonium binding domain in the pore region of Kv1.5 channels and also by threonine 505, lysine 508, and valine 512 in the S6 segment of Kv1.5 channels[17] (current numbers according to GenBank No. NM 002234: T507, K510, V514). These amino acids are also important for the stereoselective inhibition of Kv1.5 channels by bupivacaine. Mutation of T505 to valine effectively reduces stereoselectivity.[17] The corresponding position in Kv4.3 channels is valine 394. Therefore, the results of our study are in accord with the previous mutagenesis studies on Kv1.5,[17] as well as with results obtained with native I_{to}.[26] However, in contrast to bupivacaine, ropivacaine interacted with Kv4.3/KChIP2.2 channels in a stereoselective manner.[24] The lipophilicity of these local anesthetics may therefore be inversely related to their ability of stereospecific molecular inter-

action with Kv4.3/KChIP2.2 channels. Further study is needed to finally resolve this issue.

The crossing of currents under drug condition with the currents under drug free condition may be explained by a reversal of the effects of KChIP2.2 on $Kv4.3_{wt}$ channel gating.[24] A possible interaction of bupivacaine with KChIP2.2 may also explain why the block of $Kv4.3_{wt}$/KChIP2.2 developed significantly slower than block of $Kv4.3_{wt}$ channels. Because KChIP2.2 changes the inhibition of $Kv4.3_{wt}$ channels by the open pore blocker bupivacaine, it could be further hypothesized that KChIP2.2 also binds to the pore region. However, this seems less likely for several reasons.

It is well established that the N-terminus is crucial for KChIP interaction with Kv4 channels.[9,11] By impairing the movement of the N-termini to the internal mouth of the pore, KChIPs reduce N-type inactivation from the open state[33] and increase closed state inactivation, resulting from conformational changes at the internal vestibule of the pore (V-type inactivation).[33,34] This effect of KChIP can be antagonized by intracellular application of an N-terminal peptide.[35] As these changes in channel gating occur without a direct interaction of KChIP with the ion channel pore, sterical interaction of the pore blocker bupivacaine and KChIP2.2 is unlikely to occur. This view is supported by the results obtained with the Kv4.3 pore mutant V401I. The mutation V401I slows macroscopic current decline of Kv4.3/KChIP2.2 channel complexes as well as recovery from inactivation. As the current density of both $Kv4.3_{wt}$ and $Kv4.3_{V401I}$ channels is increased by coexpression with KChIP2.2, binding of KChIP2.2 to $Kv4.3_{V401I}$ channels does not seem impaired. In addition, the voltage dependence of activation and inactivation of $Kv4.3_{V401I}$ is very similar to that of $Kv4.3_{wt}$. Hence, the gating properties of the channel and of the channel complex with KChIP2.2 are only marginally influenced by this mutation, making it particularly suitable for pharmacologic studies. In contrast to $Kv4.3_{wt}$ channels, inhibition of $Kv4.3_{V401I}$ channels by bupivacaine is not reduced by coexpression with KChIP2.2, and bupivacaine does not induce a crossing of inhibited currents with control currents. Furthermore, the onset of block of $Kv4.3_{V401I}$ is not altered by coexpression with KChIP2.2. The lack of a crossing phenomenon may be explained by different inactivation time constants of $Kv4.3_{wt}$/KChIP2.2 and $Kv4.3_{V401I}$/KChIP2.2. τ_1 of current decline is significantly decreased by the local anesthetic in all channels investigated, whereas τ_2 is significantly increased by bupivacaine only in $Kv4.3_{wt}$/KChIP2.2 complexes. When comparing the absolute values of the time constants of current decline and their amplitudes (table 3), it becomes obvious that despite different inactivation time constants under control conditions, both τ_1 and τ_2 of $Kv4.3_{wt}$/KChIP2.2 and $Kv4.3_{V401I}$/KChIP2.2 current decline behave in exactly the same way under the influence of bupivacaine. The reduction of Kv4.3 inhibition caused by coexpression with KChIP2.2, therefore, is a consequence of the relatively small τ_2 value of $Kv4.3_{wt}$/KChIP2.2 under control conditions. Because KChIP2.2 binds to both $Kv4.3_{wt}$ as well as $Kv4.3_{V401I}$, the interaction of bupivacaine with the ion channel pore is unlikely to be altered by direct interaction of the local anesthetic with KChIP2.2.

The results of this study add further evidence to the model suggested previously to describe the interference of effects of amino-amide local anesthetics and KChIP subunits while acting on Kv4.3 channels.[24] Kv4.3 channels inactivate from a preopen closed state by a mechanism involving conformational changes at the internal vestibule of the pore[33,34] as well as from the open state by a mechanism involving the N-termini.[33,35] The interaction of KChIP with the N-termini impairs inactivation from the open state by preventing the channel's N-termini to interact with the internal mouth of the pore.[33] Consequently, inactivation from the preopen closed state predominates in complexes formed by Kv4 and KChIP subunits.[33] By interacting with the channel pore, bupivacaine introduces a blocked open state of Kv4.3/KChIP2.2 channels reminiscent of N-type inactivation.[29,30] Bupivacaine thus reverses KChIP2.2 effects on Kv4.3 channels by mimicking the interaction of the N-termini of the α subunit with its ion channel pore.

In summary, the amino-amide local anesthetic bupivacaine inhibited complexes formed by Kv4.3/KChIP2.2 in a concentration-dependent and reversible manner. The results of our study are consistent with the idea that bupivacaine blocks Kv4.3/KChIP2.2 channels from the open state. By influencing channel gating, KChIP2.2 indirectly altered the response of Kv4.3 channels to bupivacaine.

The authors thank Andrea Zaisser (Technician, Institute of Neuronal Signal Transduction, Center for Molecular Neurobiology, University of Hamburg, Hamburg, Germany) for cell culture; Dirk Isbrandt, M.D. (Research Group Leader), and Kathrin Sauter (Technician, both from the Institute of Neuronal Signal Transduction) for providing the Kv4.3 mutant V401I; Dirk Isbrandt, M.D., and Robert Bähring, Ph.D. (Privatdozent, Institute of Neuronal Signal Transduction), for critically reading the manuscript; Robert Bähring, Ph.D., for help with the gating model; and Olaf Pongs, Ph.D. (Director, Institute of Neuronal Signal Transduction), for continuous support.

References

1. Dixon JE, Shi W, Wang HS, McDonald C, Yu H, Wymore RS, Cohen IS, McKinnon D: Role of the Kv4.3 K+ channel in ventricular muscle: A molecular correlate for the transient outward current. Circ Res 1996; 79:659–68

2. Nerbonne JM: Molecular basis of functional voltage-gated K+ channel diversity in the mammalian myocardium. J Physiol 2000; 525:285–98

3. Näbauer M, Beuckelmann DJ, Erdmann E: Characteristics of transient outward current in human ventricular myocytes from patients with terminal heart failure. Circ Res 1993; 73:386–94

4. Kääb S, Dixon J, Duc J, Ashen D, Näbauer M, Beuckelmann DJ, Steinbeck G, McKinnon D, Tomaselli GF: Molecular basis of transient outward potassium current downregulation in human heart failure: A decrease in Kv4.3 mRNA correlates with a reduction in current density. Circulation 1998; 98:1383–93

5. Jeck C, Pinto J, Boyden P: Transient outward currents in subendocardial Purkinje myocytes surviving in the infarcted heart. Circulation 1995; 92:465–73

6. Akar FG, Wu RC, Deschenes I, Armoundas AA, Piacentino V III, Houser SR, Tomasellei GF: Phenotypic differences in transient outward K+ current of

human and canine ventricular myocytes: Insights into molecular composition of ventricular Ito. Am J Physiol Heart Circ Physiol 2004; 286:602–9

7. Rosati B, Grau F, Rodriguez S, Li H, Nerbonne JM, McKinnon D: Concordant expression of KChIP2 mRNA, protein and transient outward current throughout the canine ventricle. J Physiol 2003; 548:815–22

8. Rosati B, Pan Z, Lypen S, Wang HS, Cohen I, Dixon JE, McKinnon D: Regulation of KChIP2 potassium channel beta subunit gene expression underlies the gradient of transient outward current in canine and human ventricle. J Physiol 2001; 533:119–25

9. An WF, Bowlby MR, Betty M, Cao J, Ling HP, Mendoza G, Hinson JW, Mattson KI, Strassle BW, Trimmer JS: Modulation of A-type potassium channels by a family of calcium sensors. Nature 2000; 403:553–6

10. Guo W, Li H, Aimond F, Johns DC, Rhodes KJ, Trimmer T, Nerbonne JM: Role of heteromultimers in the generation of myocardial transient outward K+ currents. Circ Res 2002; 90:586–93

11. Bähring R, Dannenberg J, Peters HC, Leicher T, Pongs O, Isbrandt D: Conserved Kv4 N-terminal domain critical for effects of Kv channel-interacting protein 2.2 on channel expression and gating. J Biol Chem 2001; 276:23888–94

12. Kuo HC, Cheng CF, Clark RB, Lin JJ, Lin JL, Hoshijima M, Nguyen-Tran VT, Gu Y, Ikeda Y, Chu PH, Ross J, Giles WR, Chien KR: A defect in the Kv channel-interacting protein 2 (KChIP2) gene leads to a complete loss of I(to) and confers susceptibility to ventricular tachycardia. Cell 2001; 107:801–13

13. Wang S, Patel SP, Qu Y, Hua P, Strauss HC, Morales MJ: Kinetic properties of Kv4.3 and their modulation by KChIP2b. Biochem Biophys Res Commun 2002; 295:223–9

14. Kasten GW: Amide local anesthetic alterations of effective refractory period temporal dispersion: Relationship to ventricular arrhythmias. ANESTHESIOLOGY 1986; 65:61–6

15. Scott DB, Lee A, Fagan D, Bowler GM, Bloomfield P, Lundh R: Acute toxicity of ropivacaine compared with that of bupivacaine. Anesth Analg 1989; 69:563–9

16. Knudsen K, Beckman Suurkula, M, Blomberg S, Sjovall J, Edvardsson N: Central nervous and cardiovascular effects of i.v. infusions of ropivacaine, bupivacaine and placebo in volunteers. Br J Anaesth 1997; 78:507–14

17. Franqueza L, Longobardo M, Vicente J, Delpon E, Tamkun MM, Tamargo J, Snyders DJ, Valenzuela C: Molecular determinants of stereoselective bupivacaine block of hKv1.5 channels. Circ Res 1997; 81:1053–64

18. Lipka LJ, Jiang M, Tseng GN: Differential effects of bupivacaine on cardiac K channels: Role of channel inactivation and subunit composition in drug-channel interaction. J Cardiovasc Electrophysiol 1998; 9:727–42

19. Franqueza L, Valenzuela C, Eck J, Tamkun MM, Tamargo J, Snyders DJ: Functional expression of an inactivating potassium channel (Kv4.3) in a mammalian cell line. Cardiovasc Res 1999; 41:212–9

20. Gonzalez T, Longobardo M, Caballero R, Delpon E, Tamargo J, Valenzuela C: Effects of bupivacaine and a novel local anesthetic, IQB-9302, on human cardiac K+ channels. J Pharmacol Exp Ther 2001; 296:573–83

21. Gonzalez T, Arias C, Caballero R, Moreno I, Delpon E, Tamargo J, Valenzuela C: Effects of levobupivacaine, ropivacaine and bupivacaine on HERG channels: Stereoselective bupivacaine block. Br J Pharmacol 2002; 137:1269–79

22. Gonzalez T, Navarro-Polanco R, Arias C, Caballero R, Moreno I, Delpon E, Tamargo J, Tamkun MM, Valenzuela C: Assembly with the Kvbeta1.3 subunit modulates drug block of hKv1.5 channels. Mol Pharmacol 2002; 62:1456–63

23. Friederich P, Solth A, Schillemeit S, Isbrandt D: Local anaesthetic sensitivities of cloned HERG channels from human heart: Comparison with HERG/MiRP1 and HERG/MiRP1 T8A. Br J Anaesth 2004; 92:93–101

24. Friederich P, Solth A: Interaction of ropivacaine with cloned cardiac Kv4.3/KChIP2.2 complexes. ANESTHESIOLOGY 2004; 101:1347–56

25. Courtney KR, Kendig JJ: Bupivacaine is an effective potassium channel blocker in heart. Biochim Biophys Acta 1988; 939:163–6

26. Castle NA: Bupivacaine inhibits the transient outward K+ current but not the inward rectifier in rat ventricular myocytes. J Pharmacol Exp Ther 1990; 255:1038–46

27. Isbrandt D, Leicher T, Waldschutz R, Zhu X, Luhmann U, Michel U, Sauter K, Pongs O: Gene structures and expression profiles of three human KCND (Kv4) potassium channels mediating A-type currents I(TO) and I(SA). Genomics 2000; 64:144–54

28. Hamill OP, Marty A, Neher E, Sakmann B, Sigworth FJ: Improved patch-clamp techniques for high-resolution current recording from cells and cell-free membrane patches. Pflugers Arch 1981; 391:85–100

29. Armstrong CM: Inactivation of the potassium conductance and related phenomena caused by quaternary ammonium ion injection in squid axons. J Gen Physiol 1969; 54:553–75

30. Zhou M, Morais-Cabral JH, Mann S, MacKinnon R: Potassium channel receptor site for the inactivation gate and quaternary amine inhibitors. Nature 2001; 411:657–61

31. Friederich P, Benzenberg D, Urban BW: Bupivacaine inhibits human neuronal Kv3 channels in SH-SY5Y human neuroblastoma cells. Br J Anaesth 2002; 88:864–6

32. Nilsson J, Madeja M, Arhem P: Local anesthetic block of Kv channels: role of the S6 helix and the S5-S6 linker for bupivacaine action. Mol Pharmacol 2003; 63:1417–29

33. Beck EJ, Bowlby M, An WF, Rhodes KJ, Covarrubias M: Remodelling inactivation gating of Kv4 channels by KChIP1, a small-molecular-weight calcium-binding protein. J Physiol 2002; 538:691–706

34. Jerng HH, Shahidullah M, Covarrubias M: Inactivation gating of Kv4 potassium channels: molecular interactions involving the inner vestibule of the pore. J Gen Physiol 1999; 113:641–60

35. Gebauer M, Isbrandt D, Sauter K, Callsen B, Nolting A, Pongs O, Bähring R: N-type inactivation features of Kv4.2 channel gating. Biophys J 2004; 86: 210–23